J|A|C|S
ARTICLES
Published on Web 03/11/2004

Photoactivation of the Photoactive Yellow Protein: Why Photon Absorption Triggers a Trans-to-Cis Isomerization of the Chromophore in the Protein

Gerrit Groenhof,[†] Mathieu Bouxin-Cademartory,[§] Berk Hess,[‡] Sam P. de Visser,[§] Herman J. C. Berendsen,[†] Massimo Olivucci,[||] Alan E. Mark,[†] and Michael A. Robb*[,§]

Contribution from the Departments of Biophysical Chemistry and Applied Physics, University of Groningen, Nijenborg 4, 9747 AG Groningen, The Netherlands, Chemistry Department, Imperial College London, London SW7 2AZ, United Kingdom, and Dipartimento di Chimica, Università di Siena, Via Aldo Moro, I-53100 Siena, Italy

Received November 12, 2003; E-mail: mike.robb@imperial.ac.uk

Abstract: Atomistic QM/MM simulations have been carried out on the complete photocycle of Photoactive Yellow Protein, a bacterial photoreceptor, in which blue light triggers isomerization of a covalently bound chromophore. The "chemical role" of the protein cavity in the control of the photoisomerization step has been elucidated. Isomerization is facilitated due to preferential electrostatic stabilization of the chromophore's excited state by the guanidium group of Arg52, located just above the negatively charged chromophore ring. In vacuo isomerization does not occur. Isomerization of the double bond is enhanced relative to isomerization of a single bond due to the steric interactions between the phenyl ring of the chromophore and the side chains of Arg52 and Phe62. In the isomerized configuration (ground-state cis), a proton transfer from Glu46 to the chromophore is far more probable than in the initial configuration (ground-state trans). It is this proton transfer that initiates the conformational changes within the protein, which are believed to lead to signaling.

Introduction

A wide variety of organisms have evolved mechanisms to detect and respond to visible light. In many cases, the biological response is mediated by structural changes that follow photon absorption in the protein complex. The initial step in such cases is normally the photoisomerization of a highly conjugated prosthetic group. How this leads to large-scale structural changes of the whole complex is, however, poorly understood. Here, we report atomistic QM/MM simulations of the photocycle of the Photoactive Yellow Protein (PYP), a bacterial photoreceptor. The simulations uncover the detailed sequence of structural changes that follow photon absorption, including the photoisomerization of the covalently bound chromophore and the intramolecular proton transfer, which leads to the formation of the signaling state. The results of the simulations (which are consistent with experimental observations) provide detailed structural and dynamic information at a "resolution" well beyond that achievable experimentally. The "chemical role" of the protein cavity in the control of the photoisomerization has been elucidated. Thus, the key residues in the protein have been identified, and the mechanism by which they control the necessary conformational changes that lead ultimately to signal transduction in PYP has been documented.

PYP is the primary photoreceptor for the negative phototactic response of *Halorhodospira halophila*.[1,2] It has been extensivelystudied both as a model photoreceptor protein and as a structural prototype for the PAS class of signal transduction proteins.[3] Blue light induces a trans-to-cis isomerization of a double bond in the covalently bound *p*-coumaric acid chromophore[4−9] (Figure 1). In the resulting metastable state, a change in the protonation state of the chromophore triggers major conformational changes in the protein which are believed to give rise to signal transduction.[10−12] Structural studies of

[†] Dept. of Biophysical Chemistry, University of Groningen.
[‡] Micromechanics of Materials Group, Dept. of Applied Physics, University of Groningen.
[§] Imperial College London.
[||] Università di Siena.

(1) Hellingwerf, K. J.; Hendriks, J.; Gensch, T. *J. Phys. Chem. A* **2003**, *107*, 1082−1094.
(2) Sprenger, W. W.; Hoff, W. D.; Armitage, J. P.; Hellingwerf, K. J. *J. Bacteriol*. **1993**, *177*, 3096−3104.
(3) Pellequer, J. L.; Wager-Smith, K. A.; Getzoff, E. D. *Proc. Natl. Acad. Sci. U.S.A.* **1998**, *95*, 5884−5890.
(4) Hoff, W. D.; Dux, P.; Hard, K.; Devreese, B.; Nugteren-Roodzant, I. M.; Crielaard, W.; Boelens, R.; Kaptein, R.; van Beeumen, J.; Hellingwerf, K. J. *Biochemistry* **1994**, *33*, 13959−13962.
(5) Baca, M.; Borgstahl, G. E. O.; Boissinot, M.; Burke, P.; Williams, D. R.; Slater, K.; Getzoff, E. D. *Biochemistry* **1994**, *33*, 14369−14377.
(6) Borgstahl, G. E. O.; Williams, D. R.; Getzoff, E. D. *Biochemistry* **1995**, *34*, 6278−6287.
(7) Perman, B.; Šrajer, V.; Ren, Z.; Teng, T. Y.; Pradervand, C.; Ursby, T.; Bourgeois, D.; Schotte, F.; Wulff, M.; Kort, R.; Hellingwerf, K. J.; Moffat, K. *Science* **1998**, *279*, 1946−1950.
(8) Genick, U. K.; Soltis, S. M.; Kuhn, P.; Canestrelli, I. L.; Getzoff, E. D. *Nature* **1998**, *392*, 206−209.
(9) Genick, U. K.; Borgstahl, G. E.; Ng, K.; Ren, Z.; Pradervand, C.; Burke, P. M.; Šrajer, V.; Teng, T. Y.; Schildkamp, W.; McRee, D. E.; Moffat, K.; Getzoff, E. D. *Science* **1997**, *275*, 1471−1475.
(10) Xie, A.; Hoff, W. D.; Kroon A. R.; Hellingwerf, K. J. *Biochemistry* **1996**, *35*, 14671−14677.
(11) Hoff, W. D.; Xie, A.; Van Stokkum, I. H. M.; Tang, X.-J.; Gural, J.; Kroon, A. R.; Hellingwerf, K. J. *Biochemistry* **1999**, *38*, 1009−1017.

10.1021/ja039557f CCC: $27.50

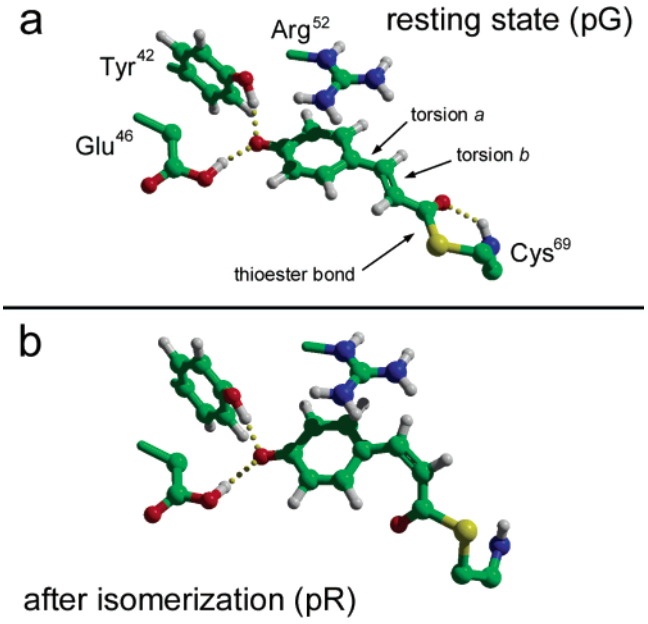

Figure 1. The *p*-coumaric acid chromophore in PYP: (a) in the resting state (pG) of the protein;[6] (b) after the absorption and isomerization (pR, last frame of a QM/MM MD trajectory). The chromophore is covalently linked to the side chain of Cys69 through a thioester bond. Its *p*-hydroxyphenyl moiety is deprotonated but stabilized by hydrogen-bonding interactions with the side chains of Tyr42 and Glu46. The negative charge is stabilized by the electrostatic interaction with the positively charged guanidinium group of Arg52. Due to steric interactions, isomerization involves not only the trans-to-cis conversion of the double bond but also flipping of the thioester linkage. The images were created with Molscript[40] and Raster3D.[41]

kinetically or cryogenically trapped intermediates[4−6] provide glimpses of structural changes that follow photoexcitation[13] but do not address the crucial question of how the protein achieves high signaling efficiency and yield no consensus about the precise sequence of events in the essentially dynamic process.

Methods

To model correctly the dynamics of the photoactivated trans-to-cis isomerization of the chromophore in PYP, the ground- and excited-state potential energy surfaces must be described accurately. The reaction starts in the excited state (S_1) but ends in the ground state (S_0), so it is essential to model the "hops" from the excited to the ground state quantum mechanically. Thus, the MD simulations were performed using a hybrid quantum mechanics/molecular mechanics (QM/MM) approach[14] including surface selection at the conical intersection seam between the excited and ground state.[15] For these calculations, a special version of Gromacs 3.0[16] with an interface to Gaussian 98[17] was used.

The chromophore was described at the CASSCF/3-21G level,[18] with an active space of 6 electrons and 6 orbitals. Strictly diabatic surface hopping was allowed only on the conical intersection hyperline of the S_1 and S_0 surfaces. The remainder of the system, consisting of the apoprotein, 4845 SPC water molecules,[19] and 6 Na^+ ions in a periodic box, was modeled with the GROMOS96 force field.[20] The $C_\alpha-C_\beta$ bond of Cys69 connecting the QM and MM subsystems was replaced by a constraint,[21] and the QM part was capped with a hydrogen atom. The force on the cap atom was distributed over the two atoms of the bond. The QM system experienced the Coulomb field of all MM atoms; Lennard-Jones interactions between MM and QM atoms were added. Our treatment resembles that used previously by Warshel and Chu[22] to study the photoisomerization of bacteriorhodopsin. Warshel and Chu[22] implemented a more sophisticated surface-hopping algorithm but used a much lower-level semiempirical QM method.[23] Also, in contrast to the work of Warshel and Chu,[22] induced dipoles were not included in the environment, as this was considered incompatible with the use of a nonpolarizable MM force field. After the isomerization, the simulations were continued classically (MM), using the chromophore force field described in previous work.[24]

The CASSCF computations are the main computational cost. At each step in the MD simulation, one must select the appropriate CI eigenvector to compute the gradient. We have used a simplified surface hop procedure which we now describe. A diabatic "hop" from S_1 to S_0 was forced when the energy gap was below a given threshold, and the CI vector indicated that a crossing had been passed. We use the symbol C_i^K to refer to the CI vector for state K at MD step i ($K = 1$ for the ground state and $K = 2$ for the excited state). Initially, C_i^2 is used to compute the gradient. When the innerproduct $C_i^2 \cdot C_{i-1}^2$ is sufficiently small and the other innerproduct $C_i^1 \cdot C_{i-1}^2$ approaches 1, then the trajectory has passed a point of an avoided or a real crossing. Provided the energy difference is less than a threshold, one assumes that the step $i-1 \rightarrow i$ has passed a point of real crossing, and one selects the eigenvector C_i^1 rather than C_i^2 to compute the gradient at step *i*. Energy is obviously conserved. Of course, such a procedure only allows surface hopping on the $n-2$-dimensional hyperline of the conical intersection. This procedure could lead to an underestimation of the crossing probability. However, our experience has shown that, in larger polyatomic systems, the conical intersection line is almost impossible to avoid because of its large dimensionality and most surface hops are, in practice, essentially diabatic.

The affinity of the chromophore for the Glu46 proton (see Figure 1) was computed as follows: In each frame of the classical MM simulation that was continued after the isomerization, the Glu46 proton was placed at 20 different positions on the line connecting the phenolate oxygen of the chromophore and the carboxylate oxygen atom of Glu46. The energy of each configuration was then calculated using the following QM/MM scheme. The contribution of the QM subsystem consisting of the chromophore and the side chains of Tyr42 and Glu46 was computed at the PM3 level.[25] To this was added the classical electrostatic contribution of the environment. In this way, the complete response of the quantum mechanical system to the position of the proton, including polarization effects, is incorporated. The procedure

(12) Rubinstenn, G.; Vuister, G. W.; Mulder, F. A. A.; Dux, P. E.; Boelens, R.; Hellingwerf, K. J.; Kaptein, R. *Nat. Struct. Biol.* **1998**, *5*, 568−570.
(13) Ren, Z.; Perman, B.; Srajer, V.; Teng, T.-Y.; Pradervand, C.; Bourgeois, D.; Schotte, F.; Ursby, T.; Kort, R.; Wulff, M.; Moffat, K. *Biochemistry* **2001**, *40*, 13788−13801.
(14) Warshel, A.; Levitt, M. *J. Mol. Biol.* **1976**, *109*, 227−249.
(15) Tully, J. C. *J. Chem. Phys.* **1990**, *93*, 1061−1071.
(16) Lindahl, E.; Hess, B.; van der Spoel, D. *J. Mol. Model.* **2001**, *7*, 306−317.
(17) Frisch, M. J.; Trucks, G. W.; Schlegel, H. B.; Scuseria, G. E.; Robb, M. A.; Cheeseman, J. R.; Zakrzewski, V. G.; Montgomery, J. A., Jr.; Stratmann, R. E.; Burant, J. C.; Dapprich, S.; Millam, J. M.; Daniels, A. D.; Kudin, K. N.; Strain, M. C.; Farkas, O.; Tomasi, J.; Barone, V.; Cossi, M.; Cammi, R.; Mennucci, B.; Pomelli, C.; Adamo, C.; Clifford, S.; Ochterski, J.; Petersson, G. A.; Ayala, P. Y.; Cui, Q.; Morokuma, K.; Malick, D. K.; Rabuck, A. D.; Raghavachari, K.; Foresman, J. B.; Cioslowski, J.; Ortiz, J. V.; Stefanov, B. B.; Liu, G.; Liashenko, A.; Piskorz, P.; Komaromi, I.; Gomperts, R.; Martin, R. L.; Fox, D. J.; Keith, T.; Al-Laham, M. A.; Peng, C. Y.; Nanayakkara, A.; Gonzalez, C.; Challacombe, M.; Gill, P. M. W.; Johnson, B. G.; Chen, W.; Wong, M. W.; Andres, J. L.; Head-Gordon, M.; Replogle, E. S.; Pople, J. A. *Gaussian 98*, revision A.7; Gaussian, Inc.: Pittsburgh, PA, 1998.
(18) Roos, B. O.; Taylor, P. R.; Siegbahn, P. E. M. *Chem. Phys.* **1980**, *48*, 157−173.
(19) Berendsen, H. J. C.; Postma, J. P. M.; van Gunsteren, W. F.; Hermans J. In *Intermolecular Forces*; Pullman, B., Ed.; D. Reidel Publishing Co.: Dordrecht, 1981; pp 331−342.
(20) Van Gunsteren, W. F.; Billeter, S. R.; Eising, A. A.; Hünenberger, P. H.; Krüger, P.; Mark, A. E.; Scott, W. R. P.; Tironi, I. G. *Biomolecular simulation: GROMOS96 manual and user guide*; BIOMOS b.v: Zürich, Groningen, 1996.
(21) Hess, B.; Bekker, H.; Berendsen, H. J. C.; Fraaije, J. G. E. M. *J. Comput. Chem.* **1997**, *18*, 1463−1472.
(22) Warshel, A.; Chu, Z. T. *J. Phys. Chem. B* **2001**, *105*, 9857−9871.
(23) Warshel, A. *Nature* **1976**, *260*, 679−683.
(24) Groenhof, G.; Lensink, M. F.; Berendsen, H. J. C.; Mark, A. E. *Proteins* **2002**, *48*, 212−219.
(25) Stewart, J. P. P. *J. Comput. Chem.* **1989**, *10*, 209−220.

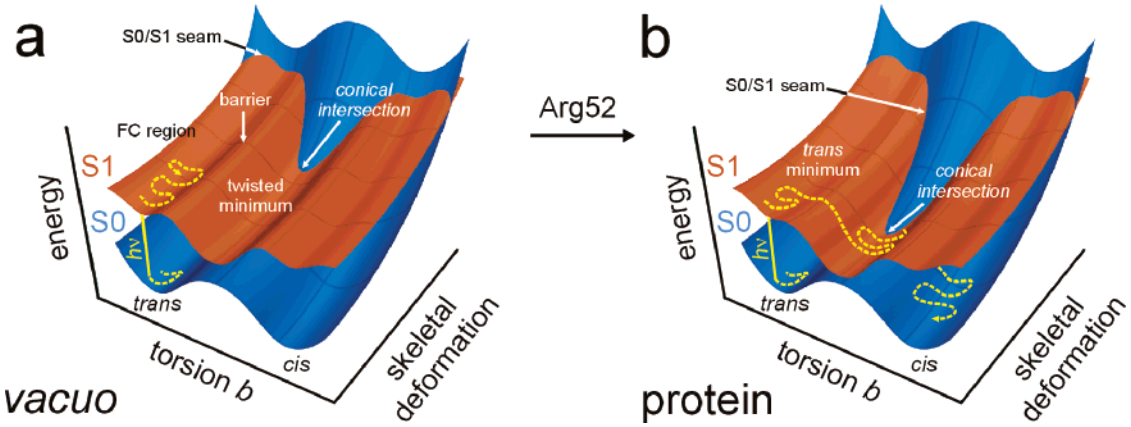

Figure 2. Potential energy surfaces of the excited and ground states of the deprotonated chromophore in the trans-to-cis isomerization coordinate (torsion *b*) and a skeletal deformation of the bonds in vacuo (a) and in the protein (b). The yellow line represents the path sampled in a typical trajectory. Motion along the torsion *b* connects the chromophore planar FC geometry to the 90° "twisted minimum". Nonradiative decay occurs along the "seam" between the surfaces (conical intersection hyperline[26]). The electrostatic field of the protein stabilizes the excited state of the twisted chromophore, moving the seam closer to the twisted S_1 minimum, and causes a decrease of the excited-state energy barrier (along torsion *b*), leading to the twisted S_1 minimum. The main contribution to the stabilization comes from the Arg52 residue, which is located on top of the chromophore ring (Figure 1).

was also performed on an extended ground-state trajectory, which served as a general reference.

In a frame for which the first analysis indicates that proton transfer would be energetically favorable, the proton was manually removed from the Glu46 side chain and added to the chromophore. This modified frame was then used as the starting structure in a next classical MM simulation, which was performed to measure the effect of the proton transfer.

Fluorescence lifetimes were determined as follows. As soon as the barrier separating the untwisted S_1 trans minimum and the global twisted S_1 minimum was passed (see Figure 2), a trajectory was no longer considered to contribute to fluorescence. The time required for passing the barrier was taken as the fluorescence lifetime of that trajectory.

Results and Discussion

Figure 2 shows a "cartoon" of the potential energy surfaces of the deprotonated chromophore, in a vacuum (left) and in the protein (right), for the ground (blue) and excited states (red) along with the path of a typical MD trajectory (yellow line). The multi-dimensional surfaces are projected onto the isomerization coordinate and the skeletal deformation coordinate. The first mode mainly involves a 180° rotation around torsion *b* (Figure 1), while the latter describes concerted contractions and expansions of the bonds between the atoms in the chromophore. The "shape" of the ground (S_0) and excited (S_1) state surfaces differ since these states have different electronic structures and charge distributions. At the S_1 global minimum configuration, where the double bond torsion angle (tosion *b* in Figure 1) is 90°, the overall negative charge is located near the thioester group in the ground state but on the phenol ring in the excited state, so the ground and excited states are affected differently by the protein environment.

The position of the "seam" of the S_1/S_0 intersection[26] of the ground and excited states (see Figure 2) controls the passage of the trajectory from the excited state to the ground state. The barrier separating the planar energy minimum, near the FC region, from the S_1 global minimum determines the efficiency of the trans-to-cis isomerization motion. In the protein environment (Figure 2b), the energy at the global minimum is lowered relative to that in vacuo (Figure 2a), resulting in (a) a decrease of the S_1-S_0 energy gap in the region of the twisted intermediate (from 80 kJ mol^{-1} in vacuo to less than 1 kJ mol^{-1} in the protein), (b) a displacement of the crossing seam closer to the global minimum, and (c) a decrease of the energy barrier separating the early planar S_1 minimum and the twisted S_1 minimum. Analysis of the protein structure suggests that the stabilization of S_1 in the protein is primarily due to the guanidium group of Arg52 that lies just above the chromophore ring (see Figure 1) and stabilizes the negative charge located on the ring in the excited state. This conjecture was tested by recomputing the S_0/S_1 energy difference at the twisted geometry (minimum on S_1), for the mutant Arg52Gly. The S_1-S_0 energy gap is increased by a factor of 10, highlighting the importance of Arg52 for the photochemical process. This finding is in agreement with the experimental observation that the mutant has a considerably longer fluorescence lifetime.[27]

In total, 14 QM/MM MD simulations were initiated at various times from a ground-state trajectory. The results are in listed Table 1. In the protein, the lifetime of the excited-state ranged from 129 to 2293 fs (third column in Table 1). The ratio of the number of successful isomerizations to the number of excited-state trajectories is ~0.3, close to the experimental quantum yield[1] of 0.35. Fitting a simple exponential ($\exp[-t/\tau]$) to the computed fluorescence lifetime data (second column of Table 1) yields a fluorescence decay time of $\tau = 200$ fs. This may be compared to time-resolved fluorescence decay measurements that show a fast decay time of 430 fs.[27] Statistically, the number of trajectories is small but nevertheless yields a consistent mechanistic picture.

Figure 3 shows a plot of the torsion angles in the tail of the chromophore during photoisomerization. There are three distinct phases: (I) the evolution on S_0, (II) excitation and evolution on S_1, and (III) decay to S_0 at the surface crossing and evolution on the S_0 surface. Immediately after the excitation ($t = 3.0$ ps, Figure 3), the chromophore decays (via bond length relaxation, see Figure 2) from the Franck−Condon region into a nearby local trans minimum on S_1. After ca. 0.4 ps ($t = 3.4$ ps, Figure 3), a shallow barrier separating this local minimum from the

(26) Robb, M. A.; Garavelli, M.; Olivucci, M.; Bernardi, F. In *Reviews in Computational Chemistry*; Lipkowitz, K. B., Boyd., D. B., Eds.; Wiley-VCH Publishers: New York, 2000; pp 15, 87−146.
(27) Mataga, N.; Chosrowjan, H.; Shibata, Y.; Imamoto, Y.; Tokunaga, F. *J. Phys. Chem. B* **2000**, *104*, 5191−5199.

Table 1. Fluorescence Lifetimes, Time of the Surface Hops (Excited-State Lifetimes), and Resulting Chromophore Conformations in 14 Different QM/MM Simulations[a]

run	fluorescence lifetime (fs)	surface hop (fs)	result
a	90	175	cis
b	141	776	cis
c	38	311	trans
d	230	1938	trans
e	63	129	trans
f	131	1185	trans
g	54	142	trans
h	384	1474	trans
i	205	571	cis
j	194	1829	cis
k	61	550	trans
l	151	1172	trans
m	734	999	trans
n	699	2293	trans

[a] The fluorescence Lifetime (second column) is defined as the time interval in which the chromophore samples the local trans S_1 minimum (Figure 2), from where fluorescence can occur. In the Methods section, it is explained how these fluorescence lifetimes were obtained from a trajectory. The excited-state lifetime (third column) is defined as the total amount of time spent in the excited state until a surface hop took place. The quantum yield was computed by dividing the number of cis results by the total number of simulations performed.

global twisted minimum (Figure 2) is crossed and the chromophore relaxes further (via rotation of the double bond, $C_2{=}C_3$, torsion *b*, by 90°) to the twisted S_1 minimum conformation. The system oscillates around this minimum (typically for 50−500 fs) until the seam is encountered (Figure 2b), and a surface hop takes the system back to the ground state ($t = 3.776$ ps). Nonradiative decay is facilitated in the protein because the "seam" lies close (Figure 2) to the reaction path sampled in the trajectory (dashed yellow line in Figure 2b).

Upon returning to the S_0 state, the chromophore relaxes back either to the trans or to a cis conformation. In the latter case, the relaxation also involves flipping of the thioester linkage (Figure 1), in which the carbonyl oxygen atom rotates 180° clockwise when viewed from the C_α of Cys69. During this process, the phenyl moiety of the chromophore remains in its original plane, the local geometry being constrained by the packing of this ring with nearby protein residues, most notably Arg52 and Phe62. Figure 1b shows the geometry of the active site after a successful isomerization. Animations of the trajectories showing the process of isomerization are available as Supporting Information.

For comparison, a series of simulations of the deprotonated chromophore in a vacuum were initiated from the same set of chromophore configurations (position and velocity) as those in the protein. In vacuo, the evolution on S_1 after photoexcitation involves the single bond $C_3{-}C_{1'}$ (torsion *a*), rather than the double bond $C_2{=}C_3$ (torsion *b*). The barrier to double bond torsion is higher than the barrier to single bond torsion, and single bond torsion leads back to the original configuration without a net conformational change. Thus, no trans-to-cis photoproduct would have been observed in the simulations in vacuo. On the time scale of the simulation, the system remains trapped in a local S_1 minimum, associated with a 90° twisted phenyl moiety (twisted $C_3{-}C_{1'}$ torsion, Figure 3, right-hand side), and does not decay (within 5 ps), because in vacuo the "seam" lies far from the path sampled in the trajectory.

In summary, the isomerization is enhanced in the protein by altering the stability of the global S_1 minimum (i.e., by moving the position of the S_1/S_0 seam and lowering the trans-to-twisted barrier on S_1, see Figure 2), and by sterically constraining the motion of the chromophore, which allows the isomerization of the double bond (torsion *b*) to be favored over isomerization of the single bond (torsion *a*). The phenyl ring of the chromophore lies stacked between the side chains of Arg52 and Phe62. These interactions significantly restrain the torsional motion of the ring about the single bond and enhance the torsional motion about the double bond. The increased population of the twisted global minimum ultimately ensures a higher quantum yield.

Following isomerization, PYP enters the third stage of the photocycle. The QM/MM MD trajectories described in the previous paragraphs are now used as the initial conditions for extended classical (ns) simulations of the system in the ground state to study this third stage. Previous classical MD simulations by Groenhof et al.[24] showed that isomerization of the chromophore can lead to the transfer of a proton to the chromophore and that this event stimulates the subsequent conformational transition (unfolding) of the protein. The validity of the initial configuration used for these simulations had, however, been questioned.[28] In the present simulations, no significant conformational changes occur in the protein within 2.0 ns after the isomerization. The hydrogen-bond network between the chromophore, Glu46, and Tyr42 (Figure 1) remains intact. The proton affinity of the chromophore, however, increases substantially. This affinity is defined as the energy difference between the protein configuration before and after the proton is transferred from the Glu46 side chain to the chromophore. Figure 4 shows the potential energy curve of the system as the proton migrates from the Glu46 side chain to the phenolate oxygen atom of the chromophore (O4′, Figure 3) in a typical protein configuration before (pG) and after (pR) photoisomerization. The difference between the two local minima, which represent the two different protonation states, is plotted as a function of time in Figure 5. Positive values imply that the transfer is energetically unfavorable. In Figures 4a and 5a, we show that, before isomerization, the energy required to transfer the proton is around 100 kJ/mol, indicating that the transfer is highly unlikely. In contrast, after isomerization (Figure 5b), the energy fluctuates around zero, becoming negative at times (as in Figure 4b). Although we have not computed the rate of proton transfer in this case, it is known from quantum dynamical simulations[29−32] that proton transfer is dominated by tunneling during fluctuations that involve equal energies for the reactant and product state, provided the distance between the donor and acceptor is sufficently small. Because the hydrogen-bonding network shown in Figure 1 remains intact throughout the simulations, the donor−acceptor distance was always optimal for proton transfer. This suggests a rapid transfer in the isomerized state. For a complete analysis of the relationship between the energy gap and the activation energy, we refer the reader to the works by Warshel.[29,30,33,34]

The energy of proton transfer after the solvent and protein had been allowed to relax in either protonation state was also

(28) Thompson, M. J.; Bashford, D.; Noodleman, L.; Getzoff, E. D. *J. Am. Chem. Soc.* **2003**, *125*, 8186−8194.
(29) Warshel, A. *Proc. Natl. Acad. Sci. U.S.A.* **1984**, *81*, 444−448.
(30) Warshel, A. *J. Phys. Chem.* **1982**, *86*, 2218−2224.
(31) Warshel, A.; Chu, Z. T. *J. Chem. Phys.* **1990**, *93*, 4003−4015.
(32) Lensink, M. F.; Mavri, J.; Berendsen, H. J. C. *J. Comput. Chem.* **1999**, *20*, 886−895.
(33) Warshel, A. *Acc. Chem. Res.* **2002**, *35*, 385−395.
(34) Warshel, A. *Q. Rev. Biophys.* **2001**, *34*, 563−679.

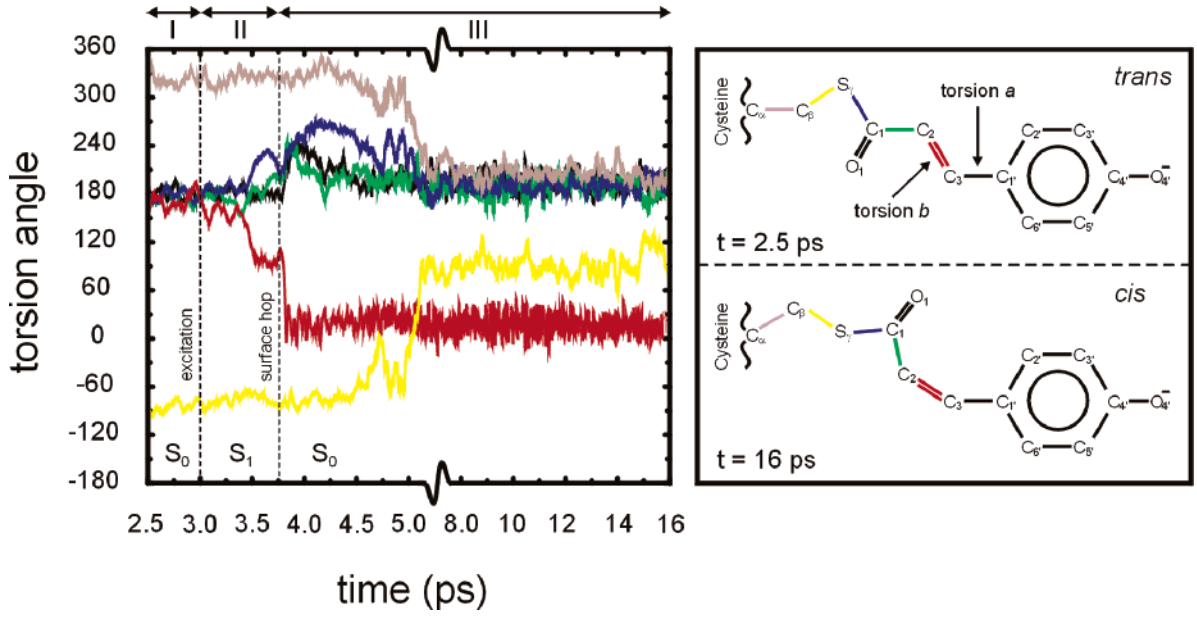

Figure 3. Behavior of the torsion angles in the tail of the chromophore during a photoisomerization simulation (run b in Table 1): $C_\alpha-C_\beta$ (brown), $C_\beta-S_\gamma$ (yellow), $S_\gamma-C_1$ (blue), C_1-C_2 (green), $C_2=C_3$ (red), and $C_3-C_{1'}$ (black). Stages: (I) before photoexcitation; (II) after photoexcitation, isomerization of the double bond (torsion *b*); and (III) on the ground state. There is no torsional change about the $C_3-C_{1'}$ single bond, and ground-state relaxation involves a rotation of 180° in opposite directions around $C_\alpha-C_\beta$ and $C_\beta-S_\gamma$, causing the thioester linkage ($C_\beta-S_\gamma-C_1$) to flip and the O_1 oxygen atom to rotate 180° clockwise as viewed from the C_α of Cys69.

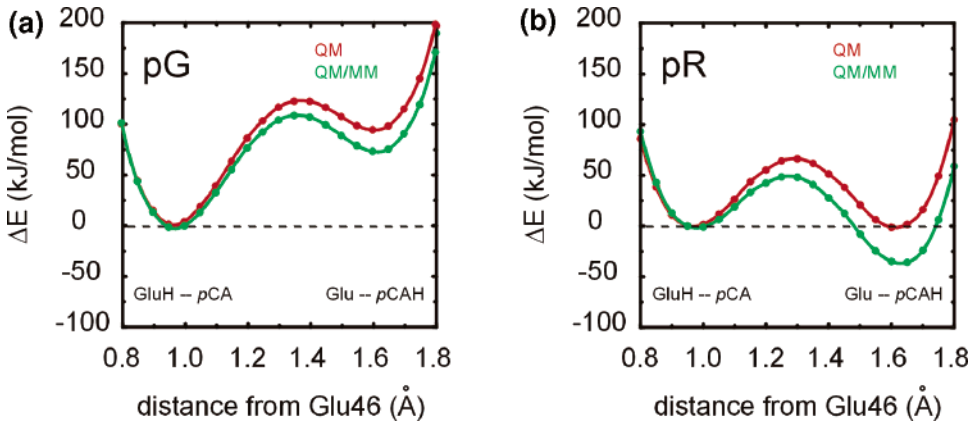

Figure 4. Potential energy profiles for a proton-transfer reaction between the Glu46 side chain and the chromophore's phenolate moiety (*p*CA, see Figure 1) in a typical protein configuration before (a) and after (b) photoisomerization of the chromophore. The reaction coordinate is defined as the distance from the donor group, the Glu46 side chain. The total distance between the donor and acceptor remained around 2.8 Å with a small fluctuation of around 0.2 Å. The offset of the curves is chosen such that the reactant minima coincide in both graphs. The green curve represents the reaction profile of the transfer in the fully hydrated protein environment (QM/MM). The red curve shows the quantum mechanical contribution to the transfer profile (QM). The latter contribution was computed by repeating the calculations on the donor−acceptor complex in vacuo. The protein stabilizes the product state with respect to the reactant state both before (pG) and after the isomerization (pR), but only after the isomerization is the proton transfer energetically favorable.

computed (see Supporting Information). Including solvent and protein relaxation, the energy was strongly positive for transfer in the trans ground state, and strongly negative for transfer in the cis ground state (after isomerization). This indicates that proton transfer from Glu46 to the chromophore becomes energetically favorable after isomerization. Despite some entropic compensation, the transfer will also be thermodynamically favored. Indeed, Yoda et al.[35] recently showed that the sign of the pK_a difference between the two groups changes from plus to minus upon going from the trans to the cis ground state, confirming our results. These authors also showed that the polarization of the environment is an essential factor in this reversal of proton affinity. We note that the concept of photoisomerization leading to changes in the pK_a's of relevant proton donors and acceptors in photoreceptor proteins had been previously proposed by both Schulten,[36,37] who suggested the pK_a change was due to the twist of the chromophore, and Warshel,[38] who suggested that the change is due to the change in the chromophore environment. In a more quantitative treatment of the third stage, one would want to compute the total free energy of the proton-transfer reaction. Because the proton transfer involves bond breaking and formation, one needs to resort to a QM/MM treatment of the system in the free energy calculation. Such an approach is far from trivial, although it has been done by others.[36] Here, we restrict ourselves to pro-

(35) Yoda, M.; Inoue, Y.; Sakurai, M. *J. Phys. Chem. B* **2003**, *107*, 14569−14575.

(36) Strabl, M.; Hong, G.; Warshel, A. *J. Phys. Chem. B* **2002**, *106*, 13333−13343.
(37) Schulten, K. *Nature* **1978**, *272*, 85−86.
(38) Warshel, A. *Photochem. Photobiol.* **1979**, *30*, 285−291.

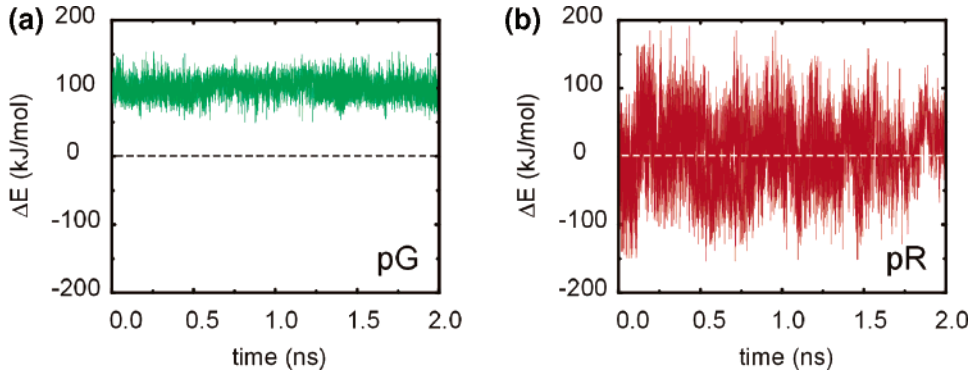

Figure 5. Affinity of the chromophore for the proton of the Glu46 side chain (Figure 1) before (a) and after (b) the isomerization.[19] The energy is plotted that is required to transfer the proton from the Glu46 side chain to the chromophore's oxygen atom ($O_{4'}$, Figure 3, right-hand side). Positive values mean that the transfer costs energy, while a negative value indicates the transfer is energetically favorable. Before the isomerization, proton transfer is always unfavorable and not likely to take place, but afterward, the energy fluctuates around zero, becoming negative very often, indicating that a proton transfer is favorable and hence more likely to occur.

viding a qualitative picture of the signal transduction mechanism rather than attempting to predict rate constants. Furthermore, as we demonstrated previously,[24] the proton transfer is not likely to be the rate-limiting step in the formation of the signaling state of the protein.

Upon transfer of the proton, the protein becomes unstable and starts to unfold. In the classical (ns) simulations that started from frames of the previous trajectories in which the proton was manually transferred, the hydrogen-bonding network between the chromophore and the side chains of Tyr42 and Glu46 breaks up within a few picoseconds. The loss of these hydrogen bonds is followed by structural changes in the protein, predominantly in the N-terminal region. These findings are in line with the conclusions of the earlier work,[24] that the transfer of the proton is the critical first step in the sequence of structural changes that lead to signaling.

Conclusion

Understanding the dynamics of subpicosecond photoactivated processes such as those that occur in PYP represents a major challenge, but is essential to elucidating how proteins have evolved to regulate such chemical processes. Here, we demonstrated that, by using a QM/MM MD strategy with explicit surface hopping, it is not only possible to reproduce experimental quantities such as quantum yields and excited-state lifetimes in PYP, but also to reveal the molecular mechanism lying at the basis of the "catalytic" activity of the protein environment on the PYP chromophore. Our results show that (i) the protein promotes trans-to-cis isomerization of the chromophore by restricting the rotation of its deprotonated *p*-hydroxyphenyl moiety; that (ii) fast nonradiative decay is enhanced in the protein by reducing the ground-excited state energy gap in a fully twisted chromophore configuration; that (iii) proton transfer is considerably facilitated in the ground-state cis-configuration relative to the initial ground-state trans-configuration; and that (iv) the proton transfer initiates conformational changes within the protein, which in turn are believed to lead to signaling. We believe that our work, but also that of others,[22,39−41] has opened up the possibility to study a wide range of photoactivated processes in proteins in atomic detail.

Acknowledgment. We thank Klaas Hellingwerf for raising our interest in this project. We also thank him and Jocelyne Vreede for stimulating discussions and their comments on this manuscript. Frans van Hoesel is acknowledged for his help in creating the images.

Supporting Information Available: An outline of alternative approaches for computing the proton-transfer energies (PDF) and two animations (MPEG) of the photoisomerization trajectories. This material is available free of charge via the Internet at http://pubs.acs.org.

JA039557F

(39) Hayashi, S.; Tajkhorshid, E.; Schulten, K. *Biophys. J.* **2003**, *85*, 1440−1449.
(40) Kraulis, P. J. *J. Appl. Crystallogr.* **1991**, *24*, 946−950.
(41) Merrit, E. A.; Bacon, D. J. *Methods Enzymol.* **1997**, *277*, 505−524.